P. A. Fletcher, and K. G. Larkin, "Direct Embedding and Detection of RST Invariant Watermarks," IH2002, Fifth International Workshop on Information Hiding, Noordwijkerhout, The Netherlands, 7-9 October, 2002.
To appear in Lecture Notes in Computer Science, Ed. Fabian Petitcolas, Springer Verlag, 2002.

Direct Embedding and Detection of RST Invariant Watermarks

Peter A. Fletcher, Kieran G. Larkin

Advanced Technology Division, Canon Information Systems Research Australia Pty, Ltd, [CISRA], 1 Thomas Holt Drive, North Ryde, NSW 2113, Australia
peter.fletcher@cisra.canon.com.au
kieran.larkin@cisra.canon.com.au

A common goal of many watermarking techniques is to produce a mark that remains detectable after the geometric transformations of Rotation, Scale and Translation; also known as RST invariance. We present a simple approach to achieving RST invariance using pixel-by-pixel addition of oscillating homogeneous patterns known as Logarithmic Radial Harmonic Functions [LRHFs]. LRHFs are the basis functions of the Fourier-Mellin transform and have perfect correlation, orthogonality, and spread-spectrum properties. Once the patterns have been embedded in an image they can be detected directly regardless of RST and with great sensitivity by correlation with the corresponding complex LRHFs. In contrast to conventional methods our approach is distinguished by the utilization of signal phase information and the absence of interpolation artifacts. Data encoding is based on the information in the relative centre positions of multiple spatially overlapping patterns.

1 Introduction

In this paper we are primarily concerned with practical watermarking schemes. A practical watermarking scheme must be resistant to the most common image editing operations if it is to be accepted by typical users. The common, non-malicious edits are rotation, scaling, shifting, cropping, blurring, filtering, contrast adjustment, colour shifting, printing, scanning, quantization and JPEG compression. The first four of these edits are known as geometric distortions or image deformations. Rather surprisingly many watermarking schemes proposed by researchers in the last half dozen years of frenetic publishing activity are vulnerable to one or more of these deformations.

One of the first systematic approaches to watermarking with resilience to rotation, scale and translation (RST) was presented by O'Ruanaidh and Pun. [1] Their method is based upon the Fourier-Mellin transform (FMT) of the Fourier magnitude of an image. The Fourier magnitude is, perhaps, one of the best known translation invariants, whilst the 2-D FMT imparts rotation and scale invariance. Prior to this work Cox[2] had proposed a watermarking scheme based upon modifying the transform (Fourier or cosine) magnitude values of the N^{th} largest values for an image. The idea being that peak ordering is unaffected by simple image deformations such as RST.

One of the earliest published methods to incorporate rotation immunity was the patent of Rhoads[3], which proposed a pattern of interlocking rings as the watermark. The underlying assumption here is that a ring is the only pattern with full rotational symmetry .

Another approach to affine image deformations is to embed an alignment pattern, or template, in an image. Perhaps the most interesting approach is based on the embedding of a near-random pattern which is periodically repeated in x and y. Such a marked image will give a large autocorrelation (AC), if suitably high-passed filtered first. The autocorrelation resembles an array of delta functions with peaks values exceeding the background image AC, so it can easily be detected even if the template itself is imperceptible. Both Kodak[4] and Philips[5, 6] have proposed AC methods.

Finally we note a technique based on the scaling and rotation of self-similar patterns. Solachidis and Pitas [7]presented a method that only requires correlation over a small range of scale factors and a small range of angles. The method is expected to be computationally intensive because of the 2-D search space with a correlation at each point.

RST invariant watermarking is a very active area of research and this introduction has omitted many of the recent publications. Our outline is not intended to be encyclopedic in it coverage, but rather to place our proposed RST method in context.

2 Fourier Mellin Basis Patterns and Invariant Functions

2.1 2-D Fourier Mellin Basis Function

In this section we introduce a remarkable family of functions by way of the Fourier-Mellin transform. In the last three decades there has been considerable research in the area of RST pattern detection, especially for military target (viz tanks and aircraft) detection. Correlation is usually the chosen mode of detection because it can often be implemented in real time using optical correlators. In 1976 Casasent and Psaltis[8] introduced the idea of invariant correlation based upon a Mellin transform. Subsequently much research has been published in this area, most notably Mendlovic et al[9], Rosen and Shamir[10], and Sheng and Shen.[11] There is also a considerable body of research in the image processing and pattern analysis literature which might be included in a full review article but has been omitted here for brevity.

The conventional viewpoint is that an image can be transformed to an RST invariant domain and then detected by correlation. An equivalent interpretation is that an image can be uniquely represented by an orthonormal series of invariant functions; and these functions are the basis functions of the 2-D Fourier-Mellin transform; also known as Logarithmic Radial Harmonic Functions (LRHFs).[1]

---

[1] Actually the Fourier-Mellin transform method of O'Ruanaidh discards the phase information of the embedded pattern, which means that it is more correct to state that the method is equivalent to the addition of a sequence of different basis functions, all centered at the spatial origin.

The 2-D Fourier-Mellin transform of a function $f(r,\theta)$ is given by

$$M(s,m)=\int_{-\pi}^{+\pi}\int_{0}^{\infty} f(r,\theta)r^{s}e^{im\theta}rdrd\theta\,. \tag{1}$$

The variable s is assumed to be complex, and m is an integer representing the circular harmonic order. It can be shown that a complete[9] orthogonal [12] sequence of functions results from setting $\Re(s)=-1$. The orthogonal 2-D Fourier –Mellin basis functions $g_{\alpha,k}(r,\theta)$ are given by

$$g_{\alpha,k}(r,\theta)=\frac{r^{i\alpha}}{r}\exp(ik\theta)\,. \tag{2}$$

It can be readily confirmed that this family of functions exhibits the required scale and rotation invariant properties we desire:

$$g_{\alpha,k}(ar,\theta+\theta_0)=Ag_{\alpha,k}(r,\theta) \tag{3}$$

where A is a complex constant independent of the polar coordinates (r,θ). The orthogonality conditions ensure that correlation based detection of such patterns is perfect (insofar as correlation results in a pure delta function peak).

2.2 Homogeneous Functions

The foregoing Fourier-Mellin approach to generating perfect RST patterns has the benefit of hindsight. Instead of proceeding by transforming an image to an RST invariant space and then embedding a pseudorandom noise pattern as described by O'Ruanaidh we initially considered the question:

Can there exist a two-dimensional pattern that has a sharp pattern when correlated with itself, and yet maintains correlation sharpness even when it is rescaled and rotated?

The answer to this question remained apparently negative for some years during our research. To begin with, we knew that a function can only have a sharp autocorrelation if it has wide spectral coverage or support. We also knew that (using the Schwarz inequality) that the maximum possible (normalized) cross-correlation for two functions occurs when the functions are identical, within a multiplicative constant. From our past research on modulation and demodulation[13] we also knew that amplitude and frequency modulated patterns [AM-FM] possess particularly attractive spatial and spectral properties. The main idea being that a pattern can be defined by its local amplitude and its local phase (or frequency). The archetypal AM-FM radial function in 2-D being

$$f(x,y)=b(r)\cos[\psi(r)] \tag{4}$$

where the amplitude $b(r)$ is real, but not necessarily positive, and the phase $\psi(r)$ can also be interpreted as an integral of the instantaneous frequency (IF). The idea that a

modulated pattern might have an IF that is essentially unchanged by scaling may seem at first counterintuitive, nevertheless it leads to a deep insight. Consider a function with spatially varying IF $q(r)$ determined by

$$2\pi q(r) = \frac{d\psi(r)}{dr}. \tag{5}$$

A function with an IF that is simply the reciprocal of the coordinate r has the immediate property of scale invariance. This surprising result follows from the rescaling of Eqn. 4:

$$f(ar) = b(ar)\cos[\psi(ar)] \tag{6}$$

combined with

$$\frac{d\psi(r)}{dr} \propto \frac{1}{r} \Rightarrow \psi(r) = \alpha \ln(r) \tag{7}$$

results in

$$\begin{aligned} f(ar) &= b(ar)\cos[\alpha \ln(r) + \alpha \ln(a)] \\ &= 2b(ar)\{\exp[i\alpha \ln(r) + i\alpha \ln(a)] + \exp[-i\alpha \ln(r) - i\alpha \ln(a)]\}. \end{aligned} \tag{8}$$

Eqn. 8 defines a function that is the sum of two separately scale invariant functions (within a constant phase) if the amplitude is a homogeneous function with a real index: $b(r) = |r|^p$.

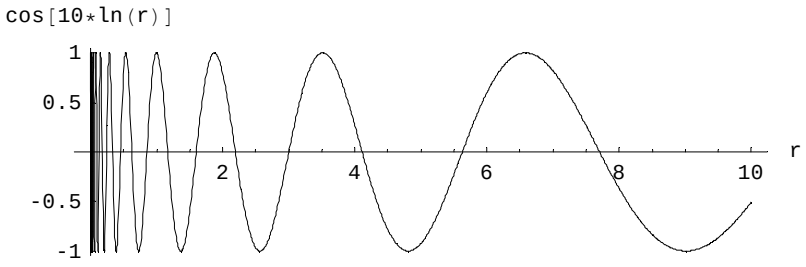

Fig. 1. Section of scale invariant function. Note the unusual singularity as $r \to 0$.

The analysis can be extended from purely radial functions by the inclusion of circular harmonics to give a result similar to Eqn. 2 except that only the real part of the function is considered:

$$\Re[g_{\alpha,k}(r,\theta)] = \frac{1}{r}\cos(\alpha \ln(r) + k\theta). \tag{9}$$

Eqn. 8 may also be expressed in complex form by the addition of the quadrature, or Hilbert conjugate, component $\hat{f}(ar) = b(ar)\sin[\alpha \ln(ar)]$ so that

$$f(ar) + i\hat{f}(ar) = b(ar)\exp[i\alpha \ln(r)]\exp[i\alpha \ln(a)] \ . \quad \textbf{(10)}$$

Recently it has been shown that the first order $(\alpha = 0, k = \pm 1)$ scale invariant transforms correspond to the Hilbert transform in 1-D and the Riesz (or spiral phase) transform in 2-D. [13]

Interestingly it seems that homogeneous functions have not been considered previously for watermarking purposes. The reason may be that the well-known real index homogeneous functions, such as r^p have very large cross-correlations with typical image functions, even though their autocorrelations have all the right properties. It transpires that complex index homogeneous functions, exemplified by Eqn. 2, have rather small cross-correlations with typical images. The full explanation of this effect is rather involved, but heuristically it is because of the rapid oscillation of the real and imaginary parts of $g_{\alpha,k}$ tend to cause cancellation with image features in the same way as pseudo random noise (PRN).

Fig. 2 shows the real and imaginary parts of the function shown in Eqn. 2 with the harmonic coefficient *k* set to zero, resulting in exact circular symmetry. Fig. 3 shows a LRHF with a spiral component $k \neq 0$.

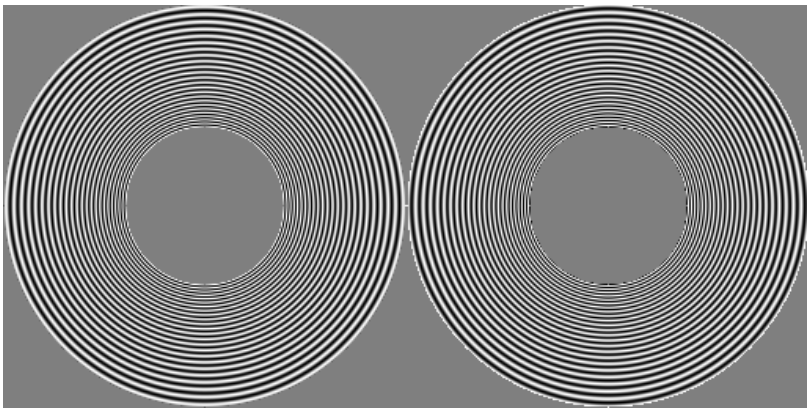

real part imaginary part

Fig. 2. Circular symmetric form of the LRHFs truncated at an inner and outer radius. Note that the central region has been set to zero to avoid aliasing of the high frequencies**.**

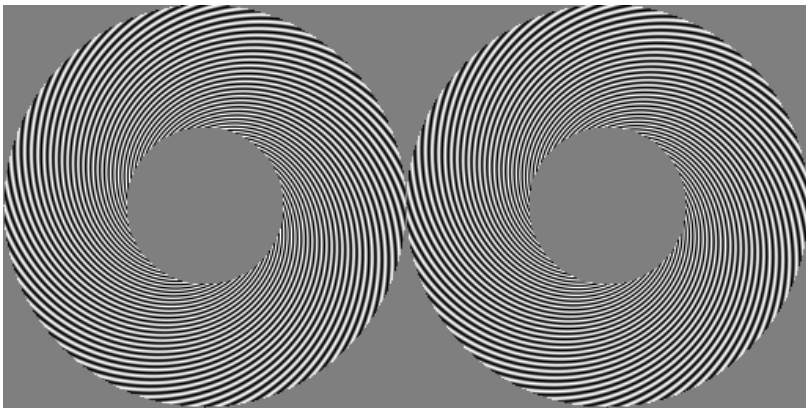

real part imaginary part

Fig. 3. The real and imaginary parts of a logarithmic radial harmonic phase function. Note how the tangential (angular) component generates an equiangular spiral. The central region has been set to zero to avoid aliasing of the high frequencies.

We now have some complex basis functions with the desired RST properties. The next section considers an additional property which supports their use in real, finite, images.

3 Orthogonality of truncated LRHFs

The first problem with using LRHFs is that they extend over all space and that they have infinitely high frequencies near the centre.[2] In practice the patterns must be limited in extent to fit in an image. The finite sampling requirement means that the maximum, non-aliased, spatial frequency is one half the sampling frequency (the Nyquist criterion). If we are to utilize these patterns they must be truncated beyond a maximum radius and below a minimum radius corresponding to the Nyquist frequency. In principle the truncation boundary may be a shape other than a circle, however we ignore this possibility here to allow the derivation of an exact orthogonality condition. In practice rectangular and other boundary shapes give near-orthogonality which is quite useable.

Firstly we consider a generalized form of the LRHF in Eqn. 2

---

[2] Ironically, singular functions have often been used as examples of pathological functions that do not have well-defined Fourier transforms. However the functions and transforms do exist as generalized functions or tempered distributions, see for example Champeney, D. C., A handbook of Fourier transforms, Cambridge University Press, Cambridge, 1987.

$$g_{p,\alpha,k}(r,\theta) = r^{p} r^{i\alpha} \exp(ik\theta) \ . \tag{11}$$

The orthogonality properties of this LRHF (over an annular region) are easily calculated because of the radial and tangential separability:

$$\begin{aligned} I_{\alpha,k,\beta,l} &= \int_{-\pi}^{+\pi} \int_{R1}^{R2} g_{p,\alpha,k}(r,\theta) g^{*}_{p,\beta,l}(r,\theta) r dr d\theta \\ &= \int_{-\pi}^{+\pi} \exp i(k-l) d\theta \int_{R1}^{R2} r^{2p} r^{i(\alpha-\beta)} r dr d\theta \ . \end{aligned} \tag{12}$$

This equation can be further simplified because the tangential (angular harmonic) component integrates to a Kronecker delta function

$$\int_{-\pi}^{+\pi} \exp i(k-l) d\theta = \delta_{k,l} = \begin{cases} 1, k = l \\ 0, k \neq l \end{cases} \ . \tag{13}$$

The radial part of the overlap integral has the following form

$$\int_{R1}^{R2} r^{2p} r^{i(\alpha-\beta)} r dr = \frac{\left(R_2^{2p+2+i(\alpha-\beta)} - R_1^{2p+2+i(\alpha-\beta)}\right)}{2p+2+i(\alpha-\beta)} \ . \tag{14}$$

Now using the original orthogonality condition $p = -1$, the magnitude squared of the overlap integral is

$$\left| I_{\alpha,k,\beta,l} \right|^2 = \delta_{k,l} \frac{\sin^2\left(\frac{[\alpha-\beta]\ln[R_2/R_1]}{2} \right)}{(\alpha-\beta)^2} \ . \tag{15}$$

Orthogonality is thus ensured for integer values of $[k,l]$ and $[\alpha,\beta]$ such that

$$\alpha - \beta = \frac{2\pi n}{\ln[R_2/R_1]}, \ n \in Z \ . \tag{16}$$

Further details about the correlation peaks function under orthogonality condition will be covered in the next few sections. For a typical digital image containing 512^2 pixels there are of the order 10^3 independent useable patterns.

4 The Remarkable Spectral Properties of LRHFs

Not only do LRHFs have unusual spatial properties, but also their spectral properties are unique. Essentially LRHFs are self-Fourier functions, but because of their scale invariance the normal Fourier scaling theorem is subverted. The continuous 2-D Fourier transform can be defined

$$F(u,v)=\int_{-\infty-\infty}^{+\infty+\infty} f(x,y)\exp(-2\pi i[ux+vy])dxdy \ . \tag{17}$$

The inverse transform similarly

$$f(x,y)=\int_{-\infty-\infty}^{+\infty+\infty} F(u,v)\exp(+2\pi i[ux+vy])dxdy \ . \tag{18}$$

It is more convenient here to work with continuous functions and FTs, but it is worth remembering that all the equations have corresponding discrete forms appropriate (although more complicated) for exact evaluation in sampled images.

It can be shown that the pure radial LRHF has the following FT, where we use the symbol $\leftrightarrow$ to indicate Fourier transformation between function pairs:

$$r^{-c} \leftrightarrow \lambda.q^{c-2},\ 0<\Re\{c\}<2 \tag{19}$$

where the spectral polar coordinates are (q,ϕ), $u=q\cos\phi$, $v=q\sin\phi$, and λ is a complex constant determined by c. Note that there is a radial inversion relation between the transform function exponents ($-c \rightarrow c-2$). The negation of the imaginary part of c is simply phase negation or complex conjugation. By partial differentiation of the above it is possible to show (informally) that the spiral LRHFs are also self-Fourier functions. Again the radial parts invert but the spiral part does not. A formal proof of these relations, being rather lengthy, is not presented here (for example see Bracewell for an outline of Bessel function methods[15]).

$$r^{-c}e^{ik\theta} \leftrightarrow \mu_c q^{c-2}e^{ik\phi},\ 0<\Re\{c\}<2 \ . \tag{20}$$

Another important frequency related property of the LRHF hinted at above is that the outer regions contain lower frequency components than the central regions. This can be formalized using the stationary phase approximation to the FT of a generalized 2-D fringe pattern. [16, 17] Treating the LRHF as an AM-FM pattern (essentially the complex form of Eqn. 4) then gives the IF (as defined by the local phase derivative) as a function of position

$$q(x,y)=\frac{1}{2\pi}\sqrt{\left(\frac{\partial\psi}{\partial x}\right)^2+\left(\frac{\partial\psi}{\partial y}\right)^2} \ . \tag{21}$$

Using the LRHF defined in Eqn. 11 we find that the IF magnitude is indeed inversely related to the radial coordinate as originally conjectured

$$q(x,y)=\frac{\sqrt{\alpha^2+k^2}}{2\pi r} \ . \tag{22}$$

A direct consequence is that the annular limitations proposed for the support practical LRHF define a maximum and a minimum frequency:

$$q_{\max} = \frac{\sqrt{\alpha^2 + k^2}}{2\pi R_{\min}}, \quad q_{\min} = \frac{\sqrt{\alpha^2 + k^2}}{2\pi R_{\max}} \ . \tag{23}$$

One fascinating consequence of this relation is that annular LRHF Fourier transform into annular LRHF in the stationary phase limit. Moreover, the inner parts of a LRHF transform into the outer parts of the FT, and vice versa. In other words the FT turns the LRHFs inside out! The significance of Eqn. 20 is that it is trivial to compute either the function or its FT directly from knowledge of the parameter *c,* allowing a shortcut in the discrete correlation computation.

5 Optimal Detection: Correlation and Translation Invariance

Correlation (or matched filtering) is known to be the optimal linear detection method under the assumption of certain noise models. Of course in watermarking the watermark is considered to be the signal and the image is the "noise". Clearly the noise is nothing like zero-mean, stationary, Gaussian noise. Following convention we ignore this intrusion of reality and pretend we have an ideal noise source!

Correlation has the important effect of introducing translation (the T in RST) invariance into the watermarking procedure. In the preceding section we have already shown how the idealized LRHFs have perfect orthogonality even after scaling and rotation.

Initially we wish to know the ideal correlation function for two untruncated LRHFs $g_{p,\alpha,k}$ and $g_{p,\beta,l}$. We use the 2-D Fourier correlation/convolution theorem (see Bracewell) [15, 18] with $\otimes\otimes$ representing the 2-D convolution operator:

$$\text{If } f(x,y) \leftrightarrow F(u,v),\ g(x,y) \leftrightarrow G(u,v) \tag{24}$$

$$\text{Then } h(x,y) = f(x,y) \otimes\otimes g(x,y) \leftrightarrow F(u,v)G^*(u,v) \ .$$

So correlation can be implemented by Fourier transforming both functions, complex conjugating one and then multiplying by the other before transforming back. For our chosen functions we find:

$$g_{p,\alpha,k}(r,\theta) = r^{p+i\alpha} e^{ik\theta} \leftrightarrow G_{p,\alpha,k}(q,\phi) = \mu_{p,\alpha} q^{-p-i\alpha-2} e^{ik\phi} \tag{25}$$

$$g_{p,\beta,l}(r,\theta) = r^{p+i\beta} e^{ik\theta} \leftrightarrow G_{p,\beta,l}(q,\phi) = \mu_{p,\beta} q^{-p-i\beta-2} e^{il\phi} \ .$$

The complex constant in each case is represented by μ. The FT of the cross-correlation is then

$$H_{p,\alpha,k,\beta,l}(u,v) = G_{p,\alpha,k}(q,\phi) G^*_{p,\beta,l}(q,\phi) = \mu_{p,\alpha}\mu_{p,\beta} q^{-2p-4-i(\alpha-\beta)} e^{i(k-l)\phi} \ . \tag{26}$$

Now we can see that the phases partly cancel when the two chosen functions are similar. Only when the functions are identical do the phases entirely cancel out. Phase cancellation is the classic condition for maximum correlation (a linear phase component can exist and merely indicates a shift between the two original functions).

At this point it is worth noting, for future reference, that several types of enhanced correlation may be used advantageously here. A phase-only correlation may be useful for detecting patterns (a phase correlation sets the magnitude of H to unity and can give a much sharper correlation peak in certain instances). Furthermore, high frequency enhanced correlation is capable of sharpening the peak. In the case where the correlated functions are identical (or scaled and rotated versions of each other) we obtain:

$$H_{p,\alpha,k,\alpha,k}(u,v) = \mu_{p,\alpha}^2 q^{-2p-4}. \tag{27}$$

The correlation peak is then a pure delta function, or a very sharp inverse cone function, depending on the real radial exponent

$$h_{p,\alpha,k,\alpha,k}(x,y) \propto \begin{cases} \delta(x,y), & p=-2 \\ \pi - \ln(r), & p=-1 \\ r^{2p+2}, & p \neq -2, p \neq -1. \end{cases} \tag{28}$$

In the latter cases of Eqn. 28 the inverse cone can be sharpened to a delta function by the use of Laplacian image enhancement (corresponding to a parabolic multiplier, q^2, in Fourier space). In the case of finite sized LRHFs we find empirically that the limit on the radial power range can be extended to $-2 \le p < 0$ at least.

Consider the quintessential scaled and rotated correlation and its FT:

$$g_{p,\alpha,k}(r,\theta) \otimes\otimes g_{p,\alpha,k}(ar,\theta+\theta_0) \leftrightarrow (\mu_{p,\alpha})^2 \left(\frac{1}{a}\right)^{p+2-i\alpha} q^{-2p-4} e^{-i(k-l)\theta_0} \tag{29}$$

In other words it is the same as the undistorted correlation in Eqn. 27 and hence the final rotated and scaled correlation is just the same as Eqn. 26 apart from a complex constant. This is precisely the correlation property we require for RST watermark detection.

It should be noted that the various integrals and FTs presented above have certain limitations related to L^2 boundedness and the existence of singular integrals, which will not be dealt upon here (see Stein[19], Champeney[14], or Calderon & Zygmund[20] for more details).

Taking the annular bounds of practical LRHFs into account modifies the result in Eq.28. The main difference being that the ideal delta spike becomes an Airy disc function, more familiar as the point spread function of a perfect annular optical imaging system. The actual energy spread is small; typically of the order of one pixel width.

5.1 Embedding Real Marks and Detecting with Complex Patterns

Having demonstrated that the LRHFs have all the required mathematical properties for RST detection we move on to an actual implementation. We are typically limited to real patterns when embedding in discrete images. We are further limited by typical

greyscale images having just 8 bits (0-255) of data per pixel. Fortunately all the preceding analysis extends easily to the case where we have a real pattern embedded in an image and we detect with a complex pattern. The main difference is a halving of the detected signal compared to the full complex correlation, as can be seen from the Fourier representation:

$$g_{p,\alpha,k}(r,\theta)\otimes\otimes\Re\left\{g_{p,\alpha,k}(ar,\theta+\theta_0)\right\} \quad \textbf{(30)}$$

$$\updownarrow$$

$$\left(\mu_{p,+\alpha}\right)^2\left(\frac{1}{a}\right)^{p+2} q^{-2p-4}e^{-ik\theta_0}\,\frac{1}{2}\left[\left(\frac{1}{a}\right)^{i\alpha}+\left(\frac{1}{a}\right)^{-i\alpha} q^{-2i\alpha}e^{-i2k\theta}\right]$$

There are two terms corresponding to the two conjugate terms in Eqn. 8. The first term in the Fourier transform is half the original (complex-complex) correlation signal. The second term is an auto-convolution term and contains frequency doubled terms which appear as a highly dispersed noise background (and in discrete systems some high frequencies will be aliased to low frequencies). The process is reminiscent of sum and difference frequency generation in AM modulators, except in 2-D. For typical image sizes (>256^2) the frequency doubled components are several orders of magnitude below the main correlation peak level and can therefore be ignored. We can conclude that scale and rotation invariant correlation is achievable for real patterns in practice.

$$\left|g_{p,\alpha,k}(r,\theta)\otimes\otimes\Re\left\{g_{p,\alpha,k}(ar,\theta+\theta_0)\right\}\right| \quad \textbf{(31)}$$

$$\cong$$

$$\frac{\left|g_{p,\alpha,k}(r,\theta)\otimes\otimes g_{p,\alpha,k}(ar,\theta+\theta_0)\right|}{2}$$

6 Proposed Embedding Algorithm

The basic idea is to add a number of LRHF patterns to an image at a near imperceptible level. Each LRHF is chosen with a different centre position but a fixed radial index α and spirality k. The relative positions of the centres can encode information in a variety of ways. In the simplest case the x and y position in a 256^2 grid can encode almost 2 bytes per pattern. It is prudent to take advantage of certain features of the human visual system to allow embedding more signal in regions where it is less visible, and less signal in particularly sensitive regions. This so-called perceptual masking is universally used in watermarking schemes. We use a very simple perceptual mask based on the local mean of the gradient magnitude to demonstrate the essential characteristics of our method, bearing in mind that more sophisticated perceptual masking could be used to further improve results. The algorithm flowchart is shown in Fig. 4.

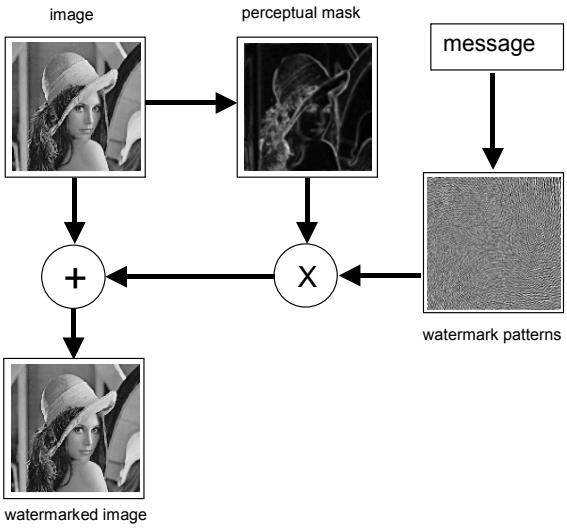

Fig. 4. Watermark Embedding Algorithm.

The effectiveness of the embedding and detection of LRHFs in typical images depends on the cross-correlation of the image with the chosen LRHF being of low magnitude and widely dispersed. In general this is difficult to estimate, however initial tests have indicated that the cross-correlation is almost always small compared to the auto-correlation. The heuristic argument for this is that LRHFs do not resemble features in typical images. The LRHFs used have both wide spatial support and wide spectral support.

7 Detection Algorithm

The first step of the detection algorithm is to undo the perceptual masking. The reason for this is that optimal detection theory predicts that the best signal detection occurs for a matched detection function. There would appear to be two possibilities; one to perceptually mask the detection function before correlation, the second, shown in Fig. 5, is to unmask the image before correlation. The first option is not actually possible to implement because it would require a different mask for each overlap integral and for each embedded pattern. The second option has the advantage, unlike the first, that the simple correlation is close to perfectly spread-spectrum, and results in a very sharp detection peak. Of course the ultimate SNR depends upon the unmasked image cross-correlation too, and this is impossible to predict in general. In practice it is not necessary to exactly undo the masking of the embedding process – experiments indicate that the unmasking step (even with a rough estimate of the mask) significantly improves peak SNR.

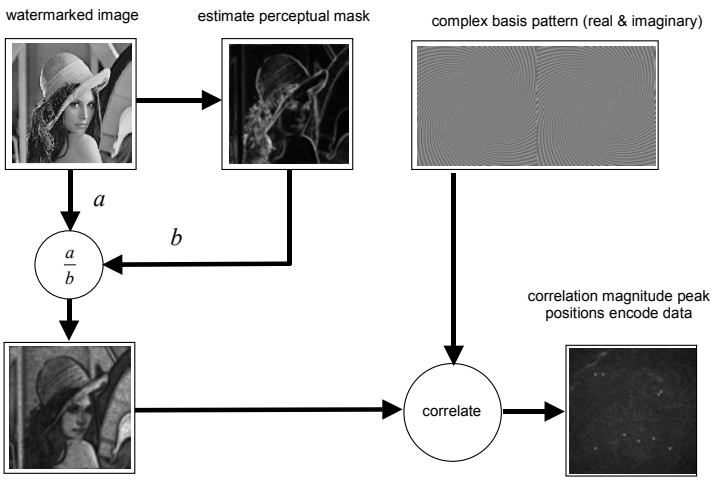

Fig. 5. Watermark detection algorithm**.**

8 Detection Results

To demonstrate the effect of RST operations on an embedded pattern we embedded 87 patterns with their centers placed in the form of the company logo CISRA. Fig. 6 shows the full sequence of results. Initially the patterns were embedded in a greyscale image of Lenna. The embedded signal has an rms of 3.6 greylevels. Applying the detection algorithm to the watermarked image recovered the logo against a background of low-level noise. The image was then rotated 17° and reduced to 80% of its original size. Applying the detection algorithm again recovered the logo against a slightly higher background noise level. Using phase-only correlation typically results in detection peaks that are localized within a few pixels with an SNR of more than 16 (peak signal/rms noise) and 2 (lowest signal peak/highest noise peak). Fig. 7 show details of the correlations peaks before and after image distortion; note that the peak energy distribution is not seriously degraded.

In real applications the number of embedded patterns can be much smaller than the above example. Embedding patterns located on a 64^2 grid requires about 12 patterns to encode 8 bytes of information, including error correction.

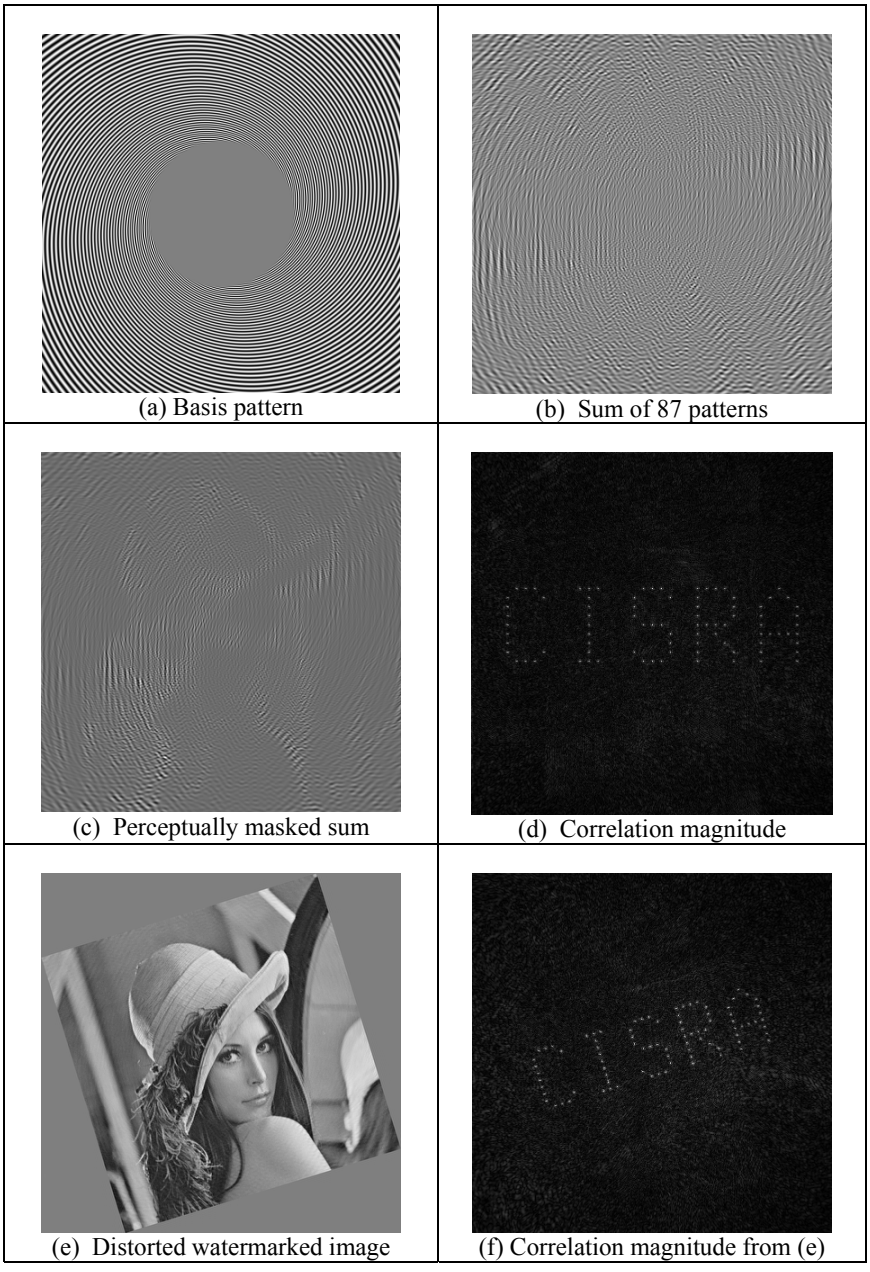

(a) Basis pattern

(b) Sum of 87 patterns

(c) Perceptually masked sum

(d) Correlation magnitude

(e) Distorted watermarked image

(f) Correlation magnitude from (e)

Fig. 6. Correlation detection results.

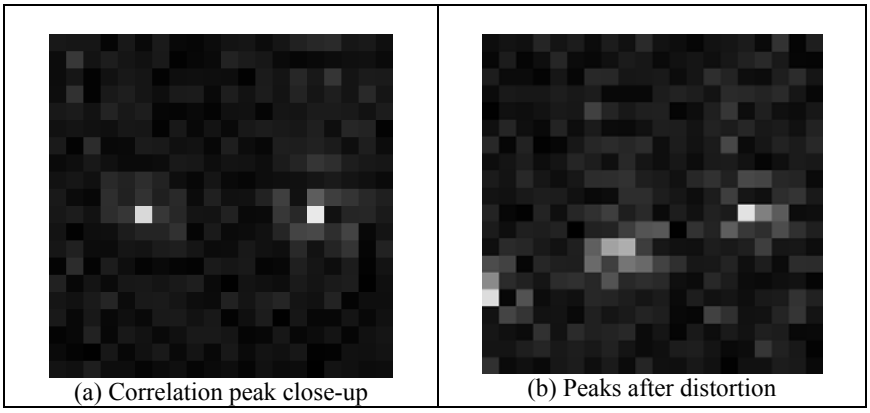

(a) Correlation peak close-up (b) Peaks after distortion

Fig. 7. Close up of correlation peaks before and after rotation-scaling distortion.

9 Performance: Resistance to Watermark Attacks

In principle a watermarking scheme based upon embedded LRHFs is completely invariant to RST and cropping. However the finite size of the patterns introduces some limitations that may be optimized for particular applications. Assuming a minimum final image size of 256^2 the method is resistant to: scaling in the range 50% to 200%, any rotation, and cropping to approx 50% of original. Simple changes to the detection search space can easily extend these ranges. Because of the spread-spectrum, wide-space nature of the patterns, they are intrinsically resistant to filtering and compression. Embedding the watermark in the luminance signal makes the mark robust to colour modifications. Random row and column deletions do reduce the correlation peaks, but not drastically. Only two Stirmark[21, 22] v3.1 attacks defeat the method. The first is the shear/aspect ratio change of more than 1%. The second is extremely low quality JPEG compression, where the image quality is unacceptable for many applications.

10 Conclusion

We have presented a family of spread-space/spread-spectrum functions that are invariant to rotation and scale essentially because of their equiangular spiral symmetry. The Logarithmic Radial Harmonic Functions have near ideal autocorrelation and orthogonality properties and can be derived from two different premises: Fourier Mellin invariance or AM-FM pattern invariance. Surprisingly the patterns have, like PRNs, very low cross-correlation with most natural images, which

makes them eminently suitable for watermarking applications. The direct embedding and detection of LRHFs avoids awkward interpolation effects (related to the log-polar transforms required by alternative RST methods) and allows encoding based on the relative centering of individual basis patterns. Like many proposed watermarking schemes the method is vulnerable to certain attacks, however malicious removal of the marks in an image of N pixels would involve at least 10^3 NlogN operations. Only the rudimentary properties and applications have been presented in this short introduction to LRHFs; much more remains to be uncovered!

References

1 O'Ruanaidh, J. J. K., and Pun, T., "Rotation, Scale and Translation Invariant Spread Spectrum Digital Image Watermarking", Sig. Proc. **66**, (3), 303-317, (1998).

2 Cox, I. J., Kilian, J., Leighton, F. T., and Shamoon, T., "Secure Spread Spectrum Watermarking For Multimedia", IEEE Transactions of Image Processing **6**, (12), 1673-1687, (1997).

3 Rhoads, G, US patent 5,636,292, "Steganography methods employing embedded calibration data", 1995.

4 Honsinger, C., and Rabbani, M., "Data Embedding Using Phase Dispersion", Eastman Kodak, 2000.

5 Linnartz, J.-P., Depovere, G., and Kalker, T., "On the Design of a Watermarking System: Considerations and Rationales," Information Hiding, Third International Workshop, IH'99, Dresden, Germany, (1999), 253-269.

6 Maes, M., Kalker, T., Haitsma, J., and Depovere, G., "Exploiting Shift Invariance to Obtain a High Payload in DigitalImage Watermarking," IEEE International Conference on Multimedia Computing and Systems, ICMCS, Florence, Italy, (1999), 7-12.

7 V.Solachidis, and Pitas, I., "Self-similar ring shaped watermark embedding in 2-D DFT domain," European Signal Processing Conf.(EUSIPCO'00), Tampere, Finland, (2000),

8 Casasent, D., and Psaltis, D., "Position, rotation, and scale invariant optical correlation", Applied Optics **15**, (7), 1795-1799, (1976).

9 Mendlovic, D., Marom, E., and Konforti, N., "Shift and scale invariant pattern recognition using Mellin radial harmonics", Opt. Comm. **67**, (3), 172-176, (1988).

10 Rosen, J., and Shamir, J., "Scale invariant pattern recognition with logarithmic radial harmonic filters", App. Opt. **28**, (2), 240-244, (1989).

11 Sheng, Y., and Shen, L., "Orthogonal Fourier Mellin moments for invariant pattern recognition", J. Opt. Soc. Am. A **11**, (6), 17481757, (1994).

12 Moses, H. E., and Prosser, R. T., "Phases of complex functions from the amplitudes of the functions and the amplitudes of the Fourier and Mellin transforms", J. Opt. Soc. Am. A **73**, (11), 1451-1454, (1983).

13 Larkin, K. G., Bone, D., and Oldfield, M. A., "Natural demodulation of two-dimensional fringe patterns: I. General background to the spiral phase quadrature transform.", J. Opt. Soc. Am. A **18**, (8), 1862-1870, (2001). http://www.physics.usyd.edu.au/~larkin/

14 Champeney, D. C., A handbook of Fourier transforms, Cambridge University Press, Cambridge, 1987.

15 Bracewell, R. N., Two-Dimensional Imaging, Prentice Hall, Englewood Cliffs, New Jersey, 1995.

16 Larkin, K. G., "Topics in Multi-dimensional Signal Demodulation", PhD. University of Sydney, 2001. http://setis.library.usyd.edu.au/~thesis/

17 Larkin, K. G., "Natural demodulation of two-dimensional fringe patterns: II. Stationary phase analysis of the spiral phase quadrature transform.", J. Opt. Soc. Am. A **18**, (8), 1871-1881, (2001).

18 Bracewell, R. N., The Fourier transform and its applications, McGraw Hill, New York, 1978.

19 Stein, E. M., Singular integrals and differentiability properties of functions, Princeton University Press, Princeton, N.J., 1970.

20 Calderon, A. P., and Zygmund, A., "On the existence of certain singular integrals", Acta Mathematica **88**, 85-139, (1952).

21 Petitcolas, F. A. P., Anderson, R. J., and Kuhn, M. G., "Attacks on copyright marking systems," Information Hiding, Second International Workshop, IH'98, Portland, Oregon, USA, (1998), 219-239.

22 Petitcolas, F. A. P., "Watermarking scheme evaluation - Algorithms need common benchmarks", IEEE Signal Processing Magazine **17**, (5), 58-64, (2000).